Dynamical Diffraction and X-Ray Standing Waves from Atomic Planes Normal to a Twofold Symmetry Axis of the Quasicrystal AlPdMn

Terrence Jach,[1] Y. Zhang,[2] R. Colella,[2] M. de Boissieu,[3] M. Boudard,[3] A. I. Goldman,[4] T. A. Lograsso,[4] D. W. Delaney,[4] and S. Kycia[5]

[1]*National Institute of Standards and Technology, Gaithersburg, Maryland 20899*
[2]*Department of Physics, Purdue University, West Lafayette, Indiana 47907*
[3]*LTPCM-ENSEEG, BP 75, 38402 St. Martin d'Hères Cédex, France*
[4]*Department of Physics and Ames Laboratory, Iowa State University, Ames, Iowa 50011*
[5]*CHESS, Cornell University, Ithaca, New York 14853*

(Received 28 August 1998)

We have observed dynamical diffraction in the $[024\bar{0}\bar{2}4]$ and $[046\bar{0}\bar{4}6]$ reflections of the icosahedral quasicrystal AlPdMn in the back-reflection geometry ($\theta_B = 90°$). The x-ray fluorescence from the Al and Pd atoms exhibits strong standing wave behavior, similar to that observed in crystalline materials. The data indicate a long-range order of each species of atoms, with the coherent positions attributable to distributions of the Al and Pd, which we compare to a centrosymmetric model. We observe deviations from the model which imply small departures from inversion symmetry along the twofold symmetry axis and from the expected coherent fractions for Al. [S0031-9007(99)08910-3]

PACS numbers: 61.44.Br, 61.10.–i

The determination of the atomic structure of quasicrystals remains one of the most important questions about these remarkable materials. Present theory is concerned with the relationship between cluster models, which give insights into growth and bonding, and planar models, which are testable by diffraction [1–4]. Even the symmetry of quasicrystals remains a major question. Measurements using isotopic [5] and isomorphic [6] contrast variation, as well as Bijvoet pairs [7], have reported centrosymmetric structures. Convergent beam electron diffraction [8] and multiple beam dynamical diffraction [9] support noncentrosymmetric structures.

Until now, the location of specific elemental species in the structure has been deduced only indirectly, for example, by the analysis of Patterson functions derived from x-ray and neutron diffraction peak intensities of single-domain samples [3] or by powder diffraction peak intensities [4]. We report here the first observations of x-ray standing waves (XSW) in an aperiodic medium—quasicrystals—and their use to test directly the positions of specific elements in the structure. In this case, the fluorescence of Al and Pd in the icosahedral quasicrystal AlPdMn was excited by standing waves formed from x-ray reflections along a twofold symmetry axis. We observe long-range elemental order of the Al and Pd in single-domain samples with a high degree of perfection. A direct comparison with theoretical elemental positions is possible for any specific reflection. The observations from our sample are only consistent with a quasicrystal structure which deviates slightly from inversion symmetry along the twofold axis.

A coherent wave field for XSW is normally visible only in crystals with a lattice regularity sufficient to demonstrate the diffraction conditions of the dynamical theory [10,11]. By monitoring the x-ray fluorescence of specific elements as the reflectivity curve is scanned in energy or diffraction angle, one can determine the coherent position of specific atomic species to high precision relative to the unit cell [12].

With the discovery of diffraction from quasicrystals [13], we know that there are periodic components of the charge density in these aperiodic materials. It is valid to ask what dynamical diffraction and XSW mean in this context. Dynamical diffraction from an aperiodic medium is possible as long as there is a periodic component in the charge density over a distance comparable to the primary extinction length in the material. It was initially shown by Berenson and Birman that a Fibonacci lattice based on a reciprocal lattice vector of the type $[h + \tau h']$, where τ is the golden mean, would give rise to dynamical effects and XSW [14].

Darwin-Prins rocking curves and representative XSW have been modeled for 1D GaAs Fibonacci superlattices [15]. The theoretical rocking curves and the x-ray fluorescence calculated in response to the XSW appear similar to those observed from crystalline materials. This can be understood in terms of the atomic distributions predicted for quasicrystals. In a quasicrystal, the distribution, as modeled by the "cut and project" method, is uniform in well-defined regions which are periodically separated from each other by physical gaps [16]. Since the standing wave technique samples only the correlation of atomic positions relative to the phase of a single Fourier component of the wave field, any such correlation (nonzero coherent fraction) gives rise to XSW effects similar to those observed in crystals. Furthermore, according to the ordering of atoms within the 6D lattice used to generate quasicrystal models in 3D, we expect that the projected positions of specific elements in the distribution are not random.

 0031-9007/99/82(14)/2904(4)$15.00

Quasicrystals are now produced with a high degree of perfection: thermodynamically stable and free from phason strain [17]. Dynamical diffraction in quasicrystals has been observed in the icosahedral quasicrystal AlPdMn as the Bormann effect by Kycia *et al.* [18]. Lee *et al.* have observed three-beam diffraction effects in quasicrystals [9].

Our experiments consisted of x-ray diffraction from highly ordered specimens of $Al_{70}Pd_{21.5}Mn_{8.5}$ grown by the Bridgman technique [19]. The specimens were sliced and polished with surfaces normal to a twofold symmetry axis of the quasicrystal. After etching the surface, Berg-Barret topographs were used to determine the regions of uniform diffraction and minimal strain from which consistent results were obtained.

The x-ray diffraction measurements were made along the twofold axis of the quasicrystal at a Bragg angle $\theta_B = 90°$ [20]. The dynamical theory of diffraction predicts that at this angle the Darwin-Prins rocking curve has an extreme angular width, which typically exceeds the mosaic spread caused by strain in most metal crystals [21,22]. The coherence of the standing waves is thus maintained even in imperfect samples. The phase shift of the standing waves was obtained by scanning the incident photon energy across the rocking curves [23].

The energy scans through the Bragg condition were performed using a symmetric Si(111) double-crystal monochromator on the X-24A beam line at the National Synchrotron Light Source. The sample was enclosed in an ultrahigh vacuum chamber. The diffracted peak intensity was monitored as photoemission current from a voltage-biased wire mesh through which the x-ray beam passed on its way to and from the crystal. The Al $K\alpha$ and Pd $L\alpha$ fluorescent radiation from the quasicrystal was observed with a SiLi detector.

Figures 1(a) and 2(a) show the rocking curves scanned in energy of the $[024\bar{0}\bar{2}4]$ and $[046\bar{0}\bar{4}6]$ reflections along a twofold axis of the quasicrystal. The energies and momentum transfers are in the ratio τ. For both reflections, a large linear background was subtracted from both the beam intensity and the fluorescence data before plotting.

The estimated values of the complex susceptibilities χ for the quasicrystal reflections were obtained from calculations of a finite atomic model described below. These were used to calculate Darwin curves as a function of energy for the reflectivity of the quasicrystal. The curves were convoluted with the Darwin curves for the Si(111) monochromator crystals, which broadened the rocking curves in energy. The solid lines shown are fits to the peaks for $\theta_B = 90°$ which required the additional convolution of a Gaussian mosaic spread of the sample. In the case of the $[024\bar{0}\bar{2}4]$ reflection, the mosaic width was 1.8 times the intrinsic width, and, for the $[046\bar{0}\bar{4}6]$ reflection, a factor of 7.4 was required.

Figures 1(b), 2(b), and 2(c) show the intensity of fluorescent radiation from spectral lines recorded during the energy scans, exhibiting pronounced x-ray standing wave effects. The characteristic minimum and maximum in the fluorescence associated with the translation of the standing wave across diffracting planes in a crystal unit cell is visible here as well. In the case of the $[024\bar{0}\bar{2}4]$ reflection, the energy at $\theta_B = 90°$ is below the Pd L-edge, so only Al $K\alpha$ fluorescent radiation is recorded. Fluorescence from the Mn atoms was not observable in our experiments owing to the low energy of the Mn L-edge, the low energy of the $L\alpha$ fluorescence emission lines, and the relatively small percentage of Mn.

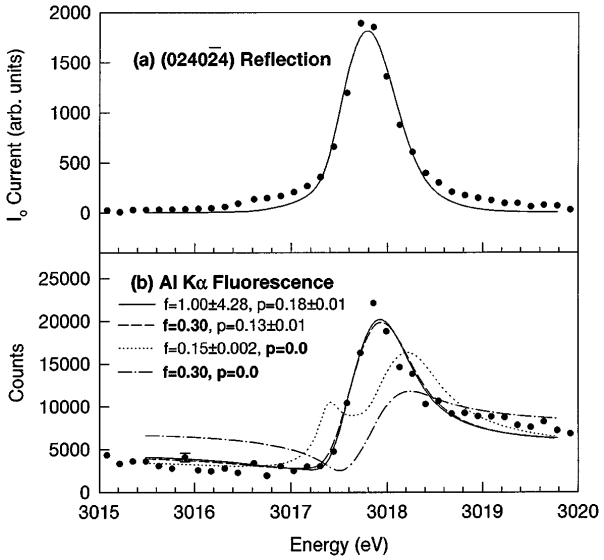

FIG. 1. (a) Diffracted peak intensity from the reflection obtained by scanning incident photon energy. The solid line is a fit to the diffraction peak (see text). (b) Al $K\alpha$ fluorescence recorded during the scan. The lines are fits obtained for f and p. Constrained variables are shown in bold. The "error bars" represent one standard deviation in the fit.

The fluorescence curves were fitted in a manner analogous to the XSW from a periodic crystal. Wave fields of the x rays were calculated by assuming a susceptibility χ using a two-beam approximation for a charge density component with a periodicity $d = 1/q$. We measured $q_{024\bar{0}\bar{2}4} = 0.48679$ Å^{-1} and $q_{046\bar{0}\bar{4}6} = 0.78842$ Å^{-1} from the energies of the reflections.

In a crystal, the fluorescence yield from an atom at a position $\vec{r}$ relative to a Miller plane responsible for a Bragg reflection [24] is given by

$$Y = C(E)\{1 + R(E) + 2\sqrt{R(E)}\, f \cos[\varphi(E) - 2\pi p]\}, \quad (1)$$

where $p = \vec{H} \cdot \vec{r}$, $\vec{H}$ is the reciprocal lattice vector, and $R(E)$ is the reflectivity as a function of the scan energy. The quantity $\varphi(E)$ is the phase of the standing wave, and $C(E)$ includes the effects of integrating the fluorescence yield down to the varying extinction depth. The coherent fraction f is the fraction of atoms of the species in the unit cell at the site $\vec{r}$. In an aperiodic quasicrystal, the coherent

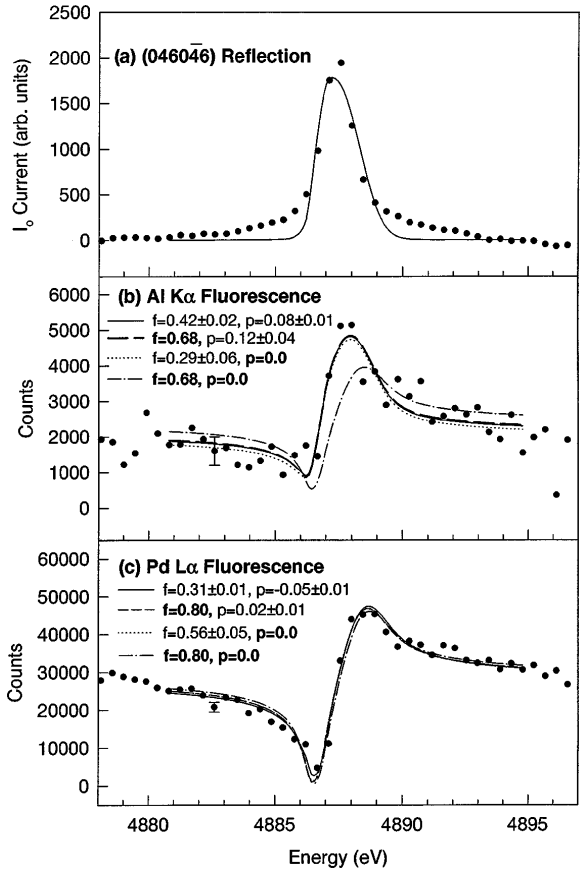

FIG. 2. (a) Diffracted peak intensity from the reflection obtained by scanning incident photon energy. The solid line is a fit to the diffraction peak (see text). (b) Al $K\alpha$ fluorescence recorded during the scan. The lines are fits obtained for f and p. Constrained variables are shown in bold. The "error bars" represent one standard deviation in the fit. (c) Pd $L\alpha$ fluorescence recorded during the scan. The lines are fits for f and p described as in (b).

fraction f indicates the fraction of atoms of each element correlated with the periodicity d of the charge density. The coherent position p indicates the centroid of that correlated distribution in units of d relative to the origin from which χ is calculated. In our centrosymmetric quasicrystal model, the origin of symmetry was chosen. The value of f associated with each reflection in the quasicrystal is a measure of the fraction of atoms of that element contributing to the reflection. The Debye-Waller factor at room temperature has a negligible effect on f in this region of phase space.

In comparing the data with theory, we used a model derived from a 6D projection [3]. It incorporated triacontahedral and spherical atomic surfaces which gave good agreement with Patterson functions determined from x-ray and neutron diffraction intensities. The projected atomic distribution was in the form of a cube 200 Å on a side. Our projection was intentionally centrosymmetric.

Assuming $\vec{q} \parallel \hat{z}$, the contribution of each atomic plane in 3D was calculated according to

$$Y = C(E)\left\{1 + R(E) + 2\sqrt{R(E)}\sum_i f_i \cos[\varphi(E) - 2\pi p_i]\right\}, \quad (2)$$

$p_i = \vec{q} \cdot \vec{z}_i$, where $f_i =$ (number of atoms of an element in plane i)/(total number of that species in the model). This calculated standing wave fluorescence yield is the equivalent to that of a single value of f and p. The fitting procedure was tested by determining the value of f and p from the model for each of the two reflections. The value of p obtained by the fit to the model fluorescence yield for each reflection was 0, as expected for explicit centrosymmetry. The values of f obtained from the model, when compared to f obtained from fits to the data, are thus tests of the model over the periodic intervals determined by each Bragg reflection.

In fitting the actual data, the same convolutions required to fit the monochromator width and mosaic broadening of the rocking curve were then applied to the XSW fits of the fluorescence curves. Test fits to synthetic data broadened by monochromator and Gaussian mosaic widths comparable to those required for our rocking curves reliably recovered f and p to better than a few percent for a wide variety of given values.

We fitted the fluorescence data in four different ways to make the most effective comparison with our model. These were (i) f and p free, (ii) f constrained to the value predicted by the model, (iii) p constrained to 0 as predicted by centrosymmetry in the model, and (iv) f and p constrained as above simultaneously. The fitting procedure in all cases included two additional parameters: an overall normalization amplitude of the fluorescence signal and a baseline offset. In all cases, the fluorescence was integrated to the primary extinction depth. The "error bars" reported correspond to variations of each variable corresponding one standard deviation in the fit criterion.

The results of fitting the Al $K\alpha$ fluorescence in the $[024\bar{0}\bar{2}4]$ reflection are shown in the plots in Fig. 1(b). The free fit of f and p results in a very broad dependence of the coherent fraction and a departure of the coherent position from 0. Constraining $f = 0.30$ as predicted for Al in the model made very little difference in the fit, as long as the coherent position was free to be nonzero. The best fits in which we constrained $p = 0$ were unable to describe accurately the XSW observed irrespective of whether f was constrained or not.

The results of fitting the Al $K\alpha$ in the $[046\bar{0}\bar{4}6]$ reflection is shown in Fig. 2(b). In the case of the Al fluorescence, the fit in which f and p are free results in a lower coherent fraction for the Al than predicted by the model. Constraining $f = 0.68$, as predicted by the model, resulted in an even larger departure from centrosymmetry. It was possible to find a fit which was constrained to centrosymmetry, $p = 0$, but this required $f = 0.29$ which is less than half the value predicted for the coherent fraction of Al in the model. Finally, a

combined constraint of $f = 0.68$ and $p = 0$ clearly gave a fit to the data which is unrealistic.

Fits to the Pd $L\alpha$ fluorescence are indicated in Fig. 2(c). In both the unconstrained and constrained cases, the fits are all remarkably similar, indicating that a centrosymmetry of the Pd atoms in the quasicrystal is strongly consistent with the data. The fits where the coherent fraction is unconstrained result in values of f that appear to be markedly lower than predicted by the model.

The distribution of Al participating in the $[024\bar{2}4]$ reflection is seen to be displaced by between 0.13 (f free) and 0.18 (f from model) of $d_{024\bar{2}4}$ from the center of the inversion symmetry. The difference in the fluorescence simultaneously obtained from Al and Pd could be understood as an offset of the Al distribution participating in the $[046\bar{4}6]$ reflection by between 0.10 (f from model) and 0.13 (f free) of $d_{046\bar{4}6}$ from the Pd distribution, which appears to be, at most, only slightly off inversion symmetry. In that case, the displacement of the two elements can be interpreted only as a lack of inversion symmetry for the quasicrystal along a twofold symmetry axis. It is possible to obtain a reasonable fit in the latter reflection when we constrain $p = 0$ for the Al. However, this requires a coherent fraction of Al atoms for this reflection which is considerably lower than predicted by the model.

In conclusion, we have demonstrated the first example of x-ray standing waves in diffraction from an aperiodic medium, an icosahedral AlPdMn quasicrystal. We are able to observe the presence of long-range order on an elemental basis, and have been able to compare the observed distribution with a model obtained from projection of a 6D lattice. The coherent position observed for Pd atoms is consistent with a centrosymmetric distribution of atoms in a model which describes accurately the intensities of major diffraction peaks. However, the fluorescence observed for Al atoms is inconsistent with inversion symmetry along the twofold rotation axis, implying deviations from centrosymmetry which have not been previously considered.

Two of the authors (T. J. and R. C.) thank S. Durbin for helpful discussions. This research was carried out in part at the National Synchrotron Light Source, which is supported by the U.S. Department of Energy. The work at Purdue University was supported by NSF Grant No. 9625585-DMR.

[1] V. Elser, Philos. Mag. B **73**, 641 (1996).
[2] W. Steurer, Mater. Sci. Forum **150**, 15 (1994).
[3] M. Boudard, M. de Boissieu, C. Janot, G. Heger, C. Beeli, H. U. Nissen, H. Vincent, R. Ibberson, M. Audier, and J. M. Dubois, J. Phys. Condens. Matter **4**, 10 149 (1992).
[4] J. L. Robertson and S. C. Moss, Z. Phys. B **83**, 391 (1991).
[5] M. Cornier-Quiquandon, R. Belissent, Y. Calvayrac, J. W. Cahn, D. Gratias, and B. Mozer, J. Non-Cryst. Solids **153**, 10 (1993).
[6] M. Boudard, M. de Boissieu, C. Janot, J. M. Dubois, and C. Dong, Philos. Mag. Lett. **64**, 197 (1991).
[7] M. de Boissieu, P. Stephens, M. Boudard, and C. Janot, J. Phys. Condens. Matter **6**, 363 (1994).
[8] M. Saito, M. Tanaka, A. P. Tsai, A. Inoue, and T. Masumoto, Jpn. J. Appl. Phys. **31**, L109 (1992).
[9] H. Lee, R. Colella, and Q. Shen, Phys. Rev. B **54**, 214 (1996).
[10] B. W. Batterman, Phys. Rev. **133**, A759 (1964); Phys. Rev. Lett. **22**, 703 (1969).
[11] S. K. Anderson, J. A. Golovchenko, and G. Mair, Phys. Rev. Lett. **37**, 1141 (1976).
[12] J. Zegenhagen, Surf. Sci. Rep. **18**, 199 (1993), and references therein.
[13] D. Shechtman, I. Blech, D. Gratias, and J. W. Cahn, Phys. Rev. Lett. **53**, 1951 (1984).
[14] R. Berenson and J. D. Birman, Phys. Rev. B **34**, 8926 (1986).
[15] J.-S. Chung and S. M. Durbin, Phys. Rev. B **51**, 14 976 (1995).
[16] E. Prince, Acta Crystallogr. Sect. A **43**, 393 (1987).
[17] S. P. Tsai, A. Inoue, Y. Yokoyama, and T. Masumoto, Philos. Mag. Lett. **61**, 9 (1990).
[18] S. W. Kycia, A. I. Goldman, T. A. Lograsso, D. W. Delaney, D. Black, M. Sutton, E. Dufresne, R. Brüning, and B. Rodericks, Phys. Rev. B **48**, 3544 (1993).
[19] D. W. Delaney, T. E. Bloomer, and T. A. Lograsso, *New Horizons in Quasicrystals: Research and Applications*, edited by A. I. Goldman, D. J. Sordelet, P. A. Thiel, and J. M. DuBois (World Scientific, Singapore, 1997), p. 45.
[20] T. Jach, S. M. Thurgate, Y. Zhang, R. Colella, A. I. Goldman, S. Kycia, M. de Boissieu, and M. Boudard, *Proceedings of the 6th International Conference on Quasicrystals*, edited by S. Takeuchi and T. Fujiwara (World Scientific, Singapore, 1998), p. 43.
[21] K. Kohra and T. Matsushita, Z. Naturforsch. **27A**, 484 (1972).
[22] A. Caticha and S. Caticha-Ellis, Phys. Rev. B **25**, 971 (1982).
[23] D. P. Woodruff, D. L. Seymour, C. F. McConville, C. E. Riley, M. D. Crapper, N. P. Prince, and R. G. Jones, Surf. Sci. **195**, 237 (1988).
[24] N. Hertel, G. Materlik, and J. Zegenhagen, Z. Phys. B **58**, 199 (1985).